doi: 10.1017/S1431927609097840
Microsc Microanal 15(Suppl 2), 2009

Scanning Confocal Electron Microscopy in a FEI Double Corrected Titan^3 TEM/STEM.

Nestor J. Zaluzec [*] Matthew Weyland[**], Joanne Etheridge[**]
[*]*Electron Microscopy Center, Mat. Science Div., Argonne National Laboratory, Argonne IL*
[**]*Monash Centre for Electron Microscopy and Dept of Materials Eng., Monash University, Vic, Australia*

Since its first implementation [1-2], the application of the Scanning Confocal Electron Microscope (SCEM) to materials and life science problems has progressed steadily albeit slowly. This progress is about to dramatically change with the deployment of electron microscopes having both probe and imaging aberration correction systems [3-4]. The correctors in these new instruments significantly increase the useable range of convergence (pre-specimen) and collection (post-specimen) angles and thus are poised to substantially improve the depth of field performance of SCEM. SCEM differs from a related method termed, 3D STEM, which employs no post specimen lenses, and has also demonstrated depth resolution in aberration corrected STEM instruments [5-6]. 3D STEM achieves its results by controlling only the prespecimen beam convergence and focus and requires a detailed knowledge of the probe-specimen interaction. In contrast, the exciting prospects for SCEM are derived from its potential to improve depth resolution, and/or in its ability to image albeit at lower resolution depth information in extremely thick specimens[1].

In this study, we have successfully implemented the SCEM mode on a FEI double corrected Titan^3 FEG-TEM/STEM at the Monash Centre for Electron Microscopy. This was accomplished by configuring the instrument as described elsewhere [2], however, unlike that previous work, this instrument is equipped with pre and post specimen aberration correctors. Here, in SCEM mode, a ~ 0.2 nm, 300 kV, 30 mr half angle incident probe was scanned across the specimen, while simultaneously the post specimen lenses were used to image the descanned probe on to a conjugate detector plane. The size and extent of the virtual SCEM aperture in this plane was controlled by the post specimen detector size and the effective magnification of the post specimen imaging system. Images were recorded simultaneously as BF/ADF pairs at the same defocus, with STEM and SCEM images recorded sequentially, owing to the need to reconfigure post specimen optics between modes.

In Figure 1 we present 2 pairs of SCEM and STEM images of a large cluster of ~ 6 nm diameter core/shell Au/Pt nanoparticles recorded at 2 different defocus values (Δf = 70 & 140 nm), the data being part of a complete through focal series (0-170 nm in 10 nm steps). In order to compare these two data sets with the same image contrast range all images were processed in the identical manner to normalize their intensity distribution. First a 15 pixel Gaussian blurred self-image was subtracted from each data set. The contrast levels were next normalized to achieve the same dynamic range and finally the background level shifted to achieve the same grey level of the average background intensity of the support film. This yielded a comparable intensity ranges in the image intensity distributions and facilitated direct comparisons, without loss of clarity or resolution.

In the STEM BF image of figure 1 (lower pair), we see the paucity of depth of field information expected from classical optics, as the effective collection angles are < 3 mr. The entire image just blurs unless taken at a specific, optimum defocus. In comparison the SCEM images (upper pair) illustrate our ability to image through the thickness of the specimen for different Δf's, allowing the determination of the depth distribution of the aggregated nanoparticles. This is most easily observed by selecting a region-of-interest in the SCEM image at defocus = 70nm (for example the small group of nanoparticles just above the magnification scale bar) and then comparing the same region with corresponding area in the other images. In the full data set (not reproduced here) it is possible to directly deduce that the region being imaged consists of planes of nanoparticle arrays upon which

clusters of nanoparticles have aggregated in the form of hollow spheroidal shells. Importantly, this has been accomplished without the need to tilt the sample or conduct a tomographic reconstruction.

We are in the process of further interrogating our SCEM image data in order to assess the ability to quantify SCEM images for 3D quantitative information. In addition, in these first experiments, the pre and post specimen imaging planes were not precisely matched. We expect to achieve considerable improvement in depth resolution with further refinement of these alignments.

References

[1] S. P. Frigo, et al, Applied Physics Letters 81, 2112 (2002).
[2] Zaluzec, N.J. , US Patent # 6,548,810 (2003); Zaluzec N.J., *Microscopy-Today Vol 6, 8 (2003)*
[3] P. D. Nellist et al., *Applied Physics Letters 89, 124105 (2006)*
[4] M. Takeguchi et al., *J Electron Microsc (Tokyo) 57, 123 (2008).*
[5] A.Y. Borisevich etal. , J Electron Microsc 55, 7–12. (2006)
[6] C. Kisielowski étal Microsc.Microanal.14,469–477, (2008)
[7] This work was supported by the US DOE Office of Science, Contract DE-AC02-06CH11357 at ANL and by the Institute for Nanosciences, Materials and Manufacturing and the MCEM at Monash University.

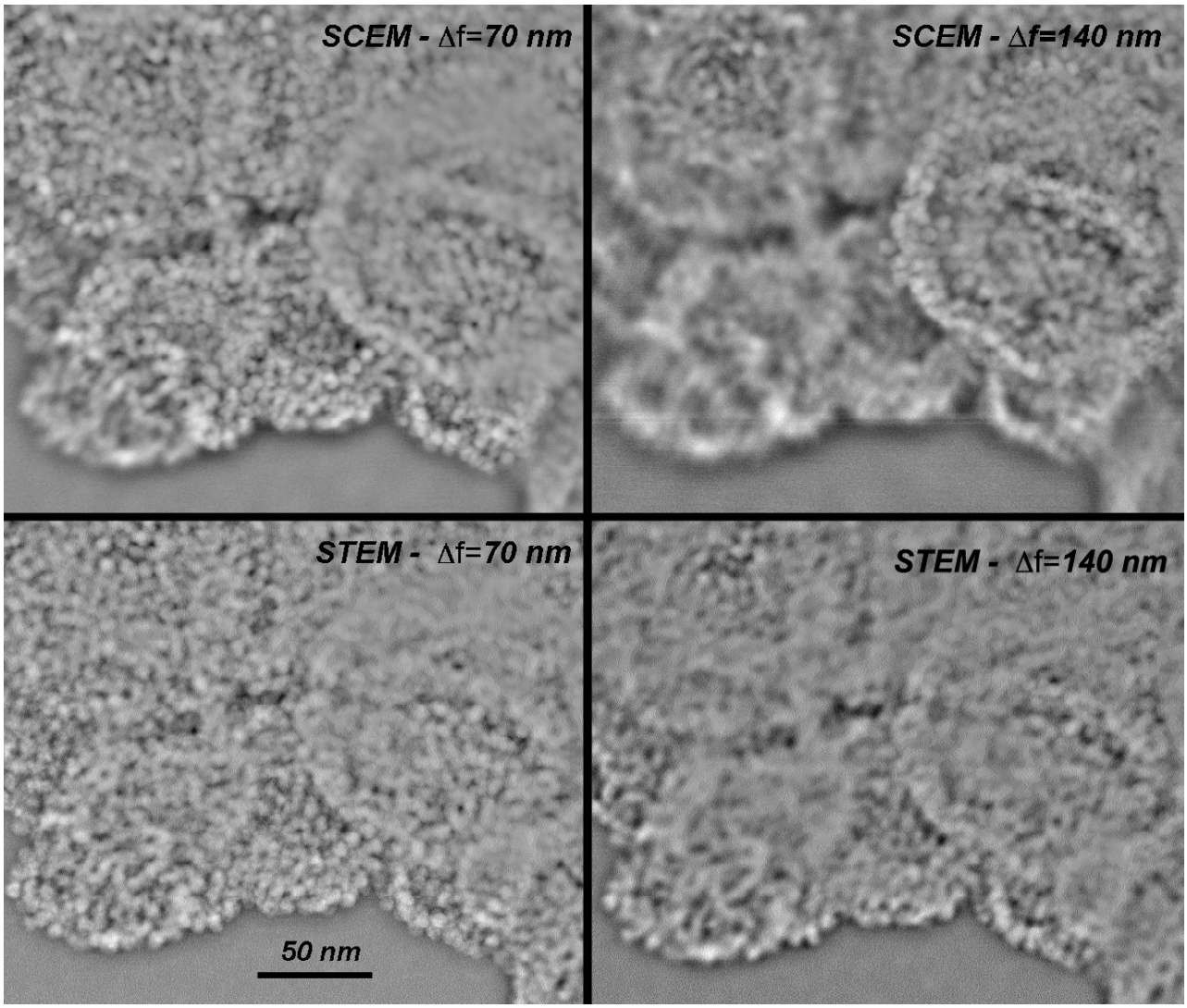

Figure 1. Comparison of SCEM and STEM images from part of a through-focal series. Note the depth identification capabilities of SCEM mode (top) relative to STEM (bottom) at the different defocus values.

https://doi.org/10.1017/S1431927609097840 Published online by Cambridge University Press